

Piezoelectric Smart Structures for Noise Reduction in a Cabin

Joongkuen Lee*, Jaehwan Kim* and Chae-Cheon Cheong*

(Received May 25, 1998)

The feasibility of piezoelectric smart structures for cabin noise problem is studied numerically and experimentally. A rectangular enclosure, one side of which is a plate while the other sides are assumed to be rigid, is considered as a cabin. A disk-shaped piezoelectric sensor and actuator are mounted on the plate structure and the sensor signal is returned to the actuator with a negative gain. An optimal design of the piezoelectric structure for active noise control of the cabin is performed. The design variables are the locations and sizes of the disk-shaped piezoelectric actuator and sensor and the actuator gain. To model the enclosure structure, a finite element method based on a combination of three dimensional piezoelectric, flat shell and transition elements is used. For the interior acoustic medium, the theoretical solution of a rectangular cavity in the absence of any elastic structures is used and the coupling effect is included in the finite element equation. The design optimization is performed at resonance and off-resonance frequencies, with the results showing a remarkable noise reduction in the cavity. An experimental verification of the optimally designed configuration confirms the feasibility of piezoelectric smart structures in resolving cabin noise problems.

Key Words : Piezoelectric Smart Structures, Cabin Noise, Finite Element Modeling, Optimal Design.

1. Introduction

Cabin noise is a significant noise problem that can be observed in buildings, automobiles, airplanes, etc. When noise source is located outside of a cavity, the external noise excites the cabin structure, and the structure radiates noise into the cavity. It is possible to control the radiated sound fields by suppressing the vibration modes of the structure that are the most efficient radiators. However, when it coincides with the resonance of the cavity it results in so-called booming noise (Oh, 1993).

In active noise control, smart structures have recently emerged as a promising technique to reduce the radiated sound field (Ko, 1996). In such structures, piezoelectric materials are widely

used as sensors and actuators, and sensor signals are returned to the actuators through a controller that essentially acts as the brain for the structure. When piezoelectric smart structures are used for the cabin noise problem, the actuators control the structures so as to reduce the radiated sound fields at a certain region, the so-called silent zone, in the cavity. The overall reduction, however, is influenced by the location and size of the piezoelectric sensors and actuators as well as the control gain. Hence, it is necessary to design the configuration of the structure optimally.

In designing piezoelectric structures for noise control, many factors affect the performance of the system. Thus, efforts to optimize these parameters are essential to achieving high performance of the system. In particular, the optimal placement of actuators has been studied for the last two decades (Clark, 1992, Wang, 1994, Varadan, 1997). However, to find the optimal configuration of the piezoelectric active structures can be difficult, because for cabin noise control, piezoelectric

* Smart Structures and System Laboratory, Department of Mechanical Engineering, Inha University, 253 Yonghyun-Dong, Nam-Ku, Incheon 402-751, KOREA.

smart structure can have different optimal configurations at different frequencies, for example, at resonance and off resonance frequencies. This means that the size and the location of the actuator as well as the sensor should be carefully configured such that when the excitation frequency is changed, the configuration cannot be changed. Another concern in optimally designing piezoelectric smart structures is that it is desirable to perform the simultaneous integrated design of the structure and control system to produce a truly optimum configuration. Recently, much research efforts have been focused on this topic (Grandi, 1989, Hale, 1985).

The approach in this paper aims to reduce cabin noise in the cavity at different frequencies by optimally designing a piezoelectric smart structure. To maximize noise reduction, not only the location and the gain voltage, but also the sizes of the actuator and sensor are optimally designed. In modeling piezoelectric smart structure with a disk-shaped piezoelectric sensor and actuator, a finite element method that uses a combination of 3-D piezoelectric, transition and shell elements is used, and for the coupling of a bounded acoustic cavity with plate structure, the modal approach is used such that the pressure fields in the cavity are

condensed out (Kim, 1997a).

Figure 1 depicts an example of the cabin noise problem we consider. The acoustic cavity is a cubic shape, in which one side of the cavity is covered with an aluminum plate, and a circular piezoelectric actuator and sensor are bonded on top of the plate. An acoustic plane wave is impinging on the plate as a noise source. The structural response is computed by using the finite element method. The pressure radiated into the cavity is then computed using the modal approach representation. An optimization technique is used to minimize the sounds in the cavity by means of rearranging the sizes, the locations and the gain. The optimally designed configuration is experimentally verified to prove its feasibility in reducing cabin noise problems.

2. Modeling and Optimization

2.1 Finite element formulation for piezoelectric smart structures

For the structural modeling, three-dimensional piezoelectric elements are used in the piezoelectric regions including their neighbors, and flat shell elements are used in the remaining part of the plate structure. To connect the shell and the three-dimensional solid elements (Fig. 2), transition elements are introduced.

The finite element equations for piezoelectric devices have already been formulated and can be written as

$$\begin{pmatrix} -\omega^2 [M] & 0 \\ 0 & 0 \end{pmatrix} + \begin{pmatrix} [K_{uu}] & [K_{u\phi}] \\ [K_{u\phi}^T] & [K_{\phi\phi}] \end{pmatrix} \begin{Bmatrix} U \\ \phi \end{Bmatrix} = \begin{Bmatrix} F + F_1 \\ Q \end{Bmatrix} \quad (1)$$

where M and K_{uu} are the mass and stiffness matrices, respectively, $K_{u\phi}$ is the piezoelectric coupling matrix and $K_{\phi\phi}$ is the dielectric stiffness matrix. U is the displacement, ϕ is the electrical potential, F is the point force on the structure, F_1

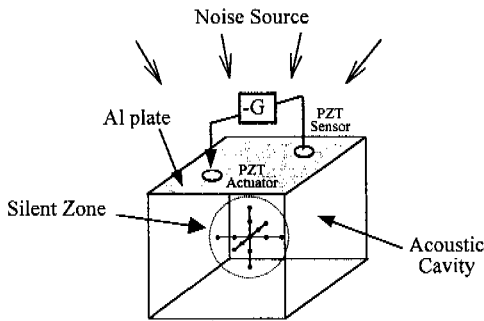


Fig. 1 Plate structure featuring piezoelectric actuator and sensor and acoustic cavity.

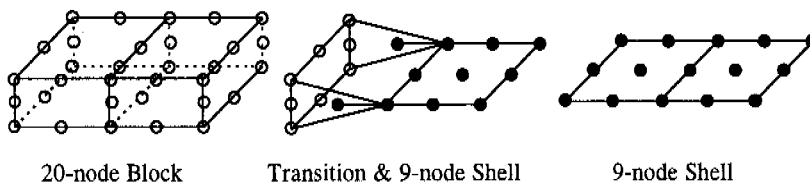


Fig. 2 Three dimensional, transition and shell elements.

is the interaction force due to the pressure in the acoustic cavity and Q is the point charge on the piezoelectric actuator. There is no distinction between the piezoelectric and structural media in applying Eq. (1) except that the piezoelectric coupling matrix and the dielectric stiffness matrix are zero in the structure. The stiffness and mass matrices of the flat shell and transition elements for the structure are already described in previous work (Kim, 1997b). The system matrix in Eq. (1) is arranged into symmetrically banded form by arranging each node's degrees of freedoms in a row. The acoustic pressure distributions applied to the top of the plate are converted into point forces, and an electrical potential is applied across the electrodes of the piezoelectric actuator. When one piezoelectric device is used as sensor, the sensor signal is directly returned to the actuator to form a closed loop by multiplying the negative gain- G , i.e.,

$$\phi_{actuator} = -G \cdot \phi_{sensor} \quad (2)$$

This constraint is difficult to implement for the following reason. $\phi_{actuator}$ is a given electric potential, say ϕ_g , while ϕ_{sensor} is a unknown value, say ϕ_u . The electric potential in Eq. (1) consists of a given value ϕ_g and unknown value ϕ_u . The electric charge corresponding to ϕ_u can be zero because it is the sensor electrode. Q is also zero for all the finite element nodes inside the piezoelectric material except the electrodes where electric potentials are specified (Kim, 1995). Since ϕ_g is given, Eq. (1) can be written as

$$\begin{pmatrix} \dots & \omega^2 \begin{bmatrix} \mathbf{M} & \mathbf{0} \\ \mathbf{0} & \mathbf{0} \end{bmatrix} + \begin{bmatrix} \mathbf{K}_{uu} & \mathbf{K}_{u\phi_u} \\ \mathbf{K}_{\phi_u u}^T & \mathbf{K}_{\phi_u \phi_u} \end{bmatrix} \end{pmatrix} \begin{Bmatrix} \mathbf{U} \\ \phi_u \end{Bmatrix} = \begin{Bmatrix} \mathbf{F} + \mathbf{F}_1 \\ \mathbf{0} \end{Bmatrix} - \begin{bmatrix} \mathbf{K}_{u\phi_g} \\ \mathbf{K}_{\phi_u \phi_g} \end{bmatrix} \begin{Bmatrix} \phi_g \end{Bmatrix} \quad (3)$$

where $\mathbf{K}_{u\phi}$ and $\mathbf{K}_{\phi\phi}$ are divided into four and two parts respectively according to ϕ_u and ϕ_g . Thus, there is no way to connect ϕ_u and ϕ_g .

A ϕ_u and ϕ_g can be evaluated by an iterative approach. Initially, the gain G is given and with the assumed actuator voltage, one can solve Eq. (3), which gives the sensor voltage ϕ_u . One ϕ_u is found, according to Eq. (2) the true actuator voltage can be calculated. When this true value does not match the previously assumed actuator

voltage, update the assumed voltage to the true value and solve Eq. (3) again. This iteration continues until the assumed actuator voltage is close to the true voltage. In practical implementations, the converged actuator voltage can be stored for the initial guess of the next finite element analysis, there by reducing the iteration number. Also, since all the coefficient matrices in Eq. (3) do not change in the iteration, these matrices can be stored to reduce the element matrix construction time. In reality, the closed loop constraint can be solved within two or three iterations. In terms of computation time, it takes 60% to 90% more time than the single finite element analysis ease to solve the constraint.

2.2 Pressure fields in the acoustic cavity

When a volume of acoustic fluid is bounded by a flexible structure, the fluid on the surface of the structure influences the motion of the structure and the normal acceleration of the structure influences the fluid field. The acoustic pressure in the cavity can be expressed as a sum of the acoustic mode shapes of the cavity (Fahy, 1985):

$$p = \sum \Lambda_{lmn} \Psi_{lmn} = \sum \Lambda_{lmn} \left(\cos \frac{l\pi x}{a} \cos \frac{m\pi y}{b} \cos \frac{n\pi z}{c} \right) \quad (4)$$

where Λ_{lmn} are unknown coefficients and l, m, n are modal integers, Ψ_{lmn} are the mode shapes of the rectangular enclosure with rigid boundary, and a, b, c are the dimensions of the box. The unknown coefficients in Eq. (4) can be found using the orthogonality condition:

$$\Lambda_{lmn} = \frac{\int_V (\omega^2 \rho_0 N_T) \cdot \Psi_{lmn} dV}{\left[k^2 - \left\{ \left(\frac{l\pi}{a} \right)^2 + \left(\frac{m\pi}{b} \right)^2 + \left(\frac{n\pi}{c} \right)^2 \right\} \right] \cdot \Lambda_{lmn}} \cdot \hat{u}_T \quad (5)$$

where Λ_{lmn} is a normalization factor. From the structural finite element equations, the interaction force due to the pressure of the cavity can be written in terms of the normal displacements. Hence, Eq. (1) can be written again as

$$\left(-\omega^2 \begin{bmatrix} \mathbf{M} + \mathbf{G} & \mathbf{0} \\ \mathbf{0} & \mathbf{0} \end{bmatrix} + \begin{bmatrix} \mathbf{K}_{uu} & \mathbf{K}_{u\phi} \\ \mathbf{K}_{\phi u}^T & \mathbf{K}_{\phi\phi} \end{bmatrix} \right) \begin{Bmatrix} \mathbf{U} \\ \phi \end{Bmatrix} = \begin{Bmatrix} \mathbf{F} \\ \mathbf{Q} \end{Bmatrix} \quad (6)$$

where

$$G = \sum_r \int_r \frac{\int_r (\rho_0 N_r \cdot \Psi_{imn}) d\Gamma}{\left[k^2 - \left\{ \left(\frac{l\pi}{a} \right)^2 + \left(\frac{m\pi}{b} \right)^2 + \left(\frac{n\pi}{c} \right)^2 \right\} \right] \cdot \Lambda_{imn}} \Psi_{imn} N_r d\Gamma$$

Once Eq. (6) is solved, the normal displacement u_r can be found so that the pressure field at any location in the cavity can be determined using Eqs. (4) and (5).

2.3 Optimization

The objective function in the optimization procedure is taken as the average pressure at the so-called silent zone in the cavity. The silent zone is composed of 13 points near the center of the cavity:

$$\min f = \frac{1}{n} \sum_{i=1}^n p_i(x_i, y_i, z_i) \tag{7}$$

where n is the number of observation points in the silent zone. The design variables are selected as:

- $b_1 = G$ (negative gain),
- $b_2 = x_1$ (x coordinate of the actuator),
- $b_3 = y_1$ (y coordinate of the actuator),
- $b_4 = x_2$ (x coordinate of the sensor),
- $b_5 = y_2$ (y coordinate of the sensor)
- $b_6 = r_1$ (radius of the actuator)
- $b_7 = r_2$ (radius of the sensor)
- $b_8 = t_1$ (thickness of the actuator)
- $b_9 = t_2$ (thickness of the sensor)

The design variables are automatically varied to achieve the goal with the variables restricted in some manner to be practical. For this, side constraints are used. A sequentially unconstrained minimization technique is used for the constraints and Powell’s method is applied to find the minimum point in each unconstrained minimum search. To allow for variations in the locations of the piezoelectric devices, an automatic mesh generation program developed in previous research (Varadan, 1997) is used. The mesh generation program together with the finite element program is linked to the optimization program.

3. Numerical Results

A cubic acoustic cavity one side of which is

covered with a square aluminum plate is considered as an example (Fig. 1). The size of the cavity is 305mm × 305mm × 305mm. The thickness of the aluminum plate is 0.8mm and the four edges of the plate are clamped to the box. From the outside of the box a plane wave with 2 Pa (100dB) peak amplitude impinges the top of the plate. Two disk-shaped piezoelectric actuator and sensor which are made of PZT-5 (Lead Zirconate Titanate) are bonded to the plate.

At first, the open loop responses at several frequencies are examined to see the behavior of the pressure distribution in the cavity. Open loop response is the response when the system is passive, the pressure at the center of the bottom of the cavity is shown in Fig. 3 as a function of noise frequency. The resonances are shown at 92, 287 and 570 Hz. For comparison, the results of SYSNOISE, a commercial FEM/BEM package, is also presented in Fig. 3. (Note that SYSNOISE does not take into account the piezoelectric devices.)

An optimal design is performed at the resonance frequencies of 92Hz and 287 Hz (Table 1). The optimal location is found to be near the corners of the plate, and the radius as well as the thickness of the piezoelectric devices are increased from the initial values. The average pressure at the silent zone in the cavity is reduced by more than 30dB at 92 and 287 Hz.

The optimal design procedure determines fixed values for the sizes and locations of the piezoelectric actuators. Thus, another attempt for verifying the robustness of the optimal result at different frequencies has been made by changing

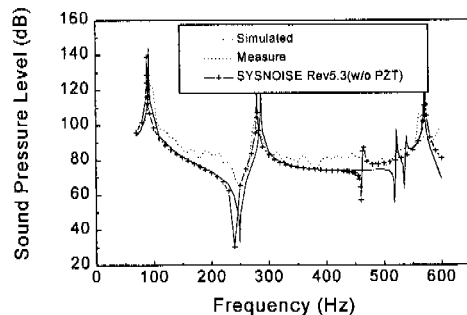
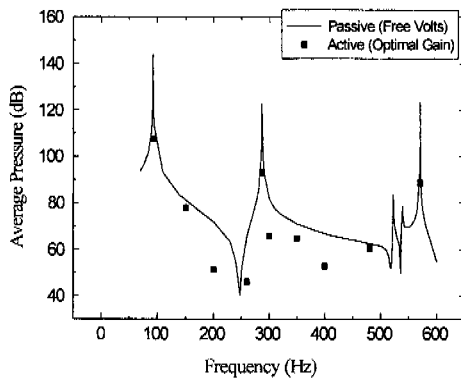


Fig. 3 Frequency response at the bottom of the cavity (no activation: passive).

Table 1 Optimal design results.

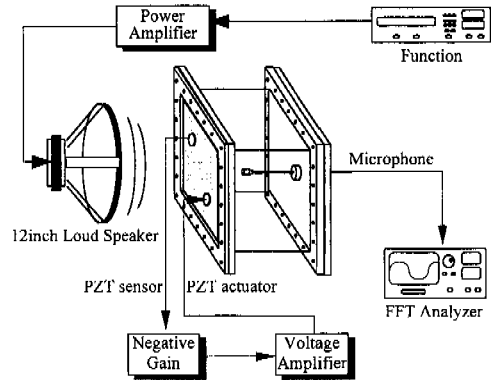
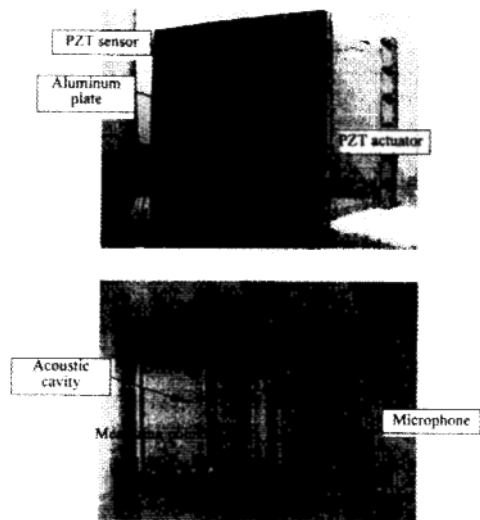
	initial		Optimal	
	92 Hz	287 Hz	92 Hz	287 Hz
$b_1(G)$	0	0	3.55	1.22
$b_2(x_1)$	100 mm	100 mm	99.3 mm	66.9 mm
$b_3(y_1)$	100 mm	100 mm	119.3 mm	68.5 mm
$b_4(x_2)$	200 mm	200 mm	204.9 mm	236.5 mm
$b_5(y_2)$	200 mm	200 mm	193.0 mm	233.1 mm
$b_6(r_1)$	10 mm	10 mm	13.5 mm	13.7 mm
$b_7(r_2)$	10 mm	10 mm	13.4 mm	13.4 mm
$b_8(t_1)$	1 mm	1 mm	1.33 mm	1.33 mm
$b_9(t_2)$	1 mm	1 mm	1.33 mm	1.32 mm
Ave. Pressure (dB)	143.9	122.9	109.2	93.1

**Fig. 4** Robustness of optimal design result at different frequencies.

the excitation frequency from 100 to 600 Hz, with the optimal configuration at 287 Hz. The actuator gain is optimally searched at each frequency. Figure 4 represents the difference between the passive response (no gain applied) and the active results (with optimal gain). In conclusion, when the excitation frequency is changed, by optimally adjusting the gain, a significant reduction can be achieved up to 400 Hz.

4. Experimental Results

An experimental verification for the optimally designed configuration was performed. The

**Fig. 5** Schematic diagram of the experimental apparatus.**Fig. 6** Photograph of the piezoelectric smart structure and acoustic cavity.

acoustic cavity is made with five acrylic thick sheets of 2 cm thick, and one side of the cavity is covered with 0.8 mm thin aluminum plate. A disk-shaped piezoelectric sensor and actuator are mounted on the plate. Figures 5 and 6 depict the configuration of the experimental apparatus. The aluminum plate is fixed with bolts and the cavity box is assured to have no leaks. The sound level inside the cavity is measured by a microphone through a small hole in the bottom of the cavity and a loudspeaker generates sound pressure from outside of the enclosure.

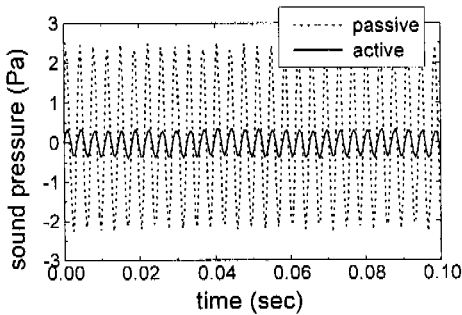
The piezoelectric sensor signal is passed through a phase shifter and amplifier, and retur-

Table 2 Sound pressure in the silent zone: measured (95 Hz, 276 Hz).

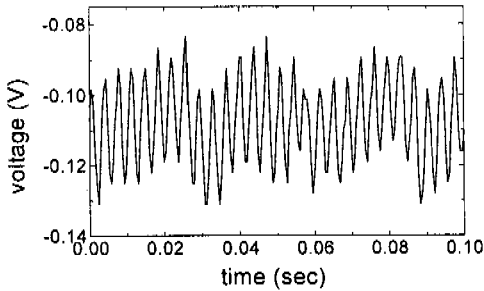
	95 Hz		276 Hz	
	Passive	Active	Passive	Active
Point 1 (dB)	122.9	110.1	97.2	89.2
Point 2 (dB)	123.1	105.6	97.4	93.8
Point 3 (dB)	123.3	110.1	98.3	84.5
Point 4 (dB)	123.5	109.8	99.5	76.4
Point 5 (dB)	123.6	112.5	100.1	81.3
Ave. Pressure (dB)	123.3	109.6	98.5	85.0

Table 3 Sound pressure in the silent zone: measured (562 Hz, 200 Hz).

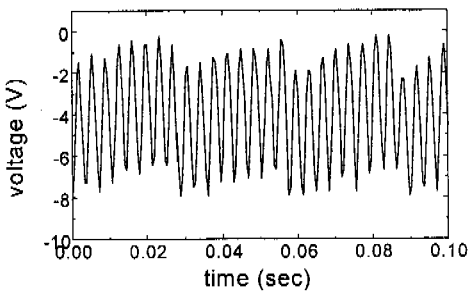
	562 Hz		200 Hz	
	Passive	Active	Passive	Active
Point 1 (dB)	104.1	101.1	82.1	80.2
Point 2 (dB)	99.2	96.2	82.9	81.4
Point 3 (dB)	85.1	81.9	83.7	82.6
Point 4 (dB)	94.1	88.4	84.1	73.7
Point 5 (dB)	101.2	80.5	84.6	77.2
Ave. Pressure (dB)	96.7	89.6	83.5	79.0



(a) Sound pressure at point 3

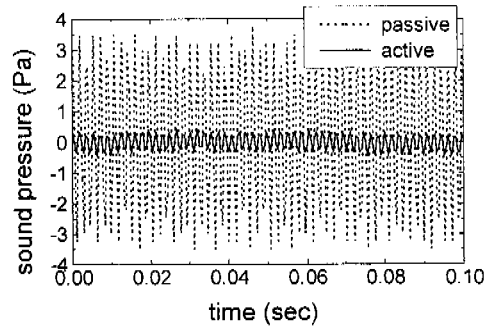


(b) Sensor signal

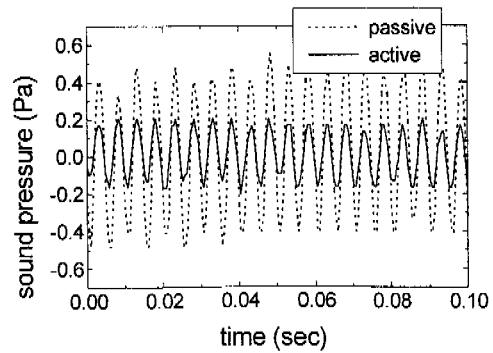


(c) Actuator input voltage

Fig. 7 Experimental results at 276Hz.



(a) Sound pressure at point 5 (562Hz)



(b) Sensor pressure at point 5 (200Hz)

Fig. 8 Experimental results (562Hz, 200Hz).

ned to the piezoelectric actuator. The pressure at the center of the bottom of the cavity is shown in Fig. 3, which matches quite well with the computational results. To verify the optimal design results, the sound pressure level is measured at five selected points and the level is averaged (Fig. 6). Table 2 shows the measured

sound pressure levels at resonance frequencies, 95 and 276Hz with the optimally designed configuration at 287Hz. The average pressures are reduced by more than 13.7dB and 13.5dB at 95Hz and 276Hz, respectively, in comparison with the passive system.

Figure 7(a) shows the time signals of the sound pressure levels measured when the actuator is activated (active) and not activated (passive). Figure 7(b) and (c) are the sensor and actuator signals at 276Hz. These results prove that the actuation voltage, in other words the feedback gain, is not high when the closed loop system is in steady state.

Table 3 represents the sound pressure levels measured at off-resonances 200Hz and 562Hz with the same configuration described previously. The averaged pressure level is reduced 4.5 to 7dB at resonance frequencies. Figure 8(a) and (b) show the time signals of the sound pressures at 562 and 200Hz, which are off-resonance. The actuator gain is not high either.

5. Conclusions

The optimal design of piezoelectric smart structures coupled with an acoustic cavity was studied to achieve a silent zone in the cavity. A finite element method which uses a combination of three dimensional piezoelectric, flat shell and transition finite elements is adopted to model the piezoelectric active structure. The shape of the acoustic cavity is cubic and the modal approach was used to represent the pressure fields in the cavity. Without any activation, the average pressure in the cavity at different frequencies is investigated, and a comparison was made with the experimental results. The comparison shows that the pressure distribution in the cavity computed by the finite element analysis approach is correct.

The optimization procedure was performed to reduce the average pressure at a silent zone in the cavity. The objective function is the average pressure in the cavity and the design variables are the locations and sizes of the piezoelectric sensor and actuator as well as the gain. The optimal location tends to be near the corners of the plate,

and more than 30dB noise reduction is achieved at resonance frequencies of the coupled system. To verify the robustness of the optimally designed configuration, the configuration found at 287Hz is used to examine the noise reduction at different frequencies. Up to 400Hz, a remarkable noise reduction can be achieved by choosing proper gain at each frequency.

Experimental verification of the optimally designed configuration shows that the average pressure is reduced by 14dB at the first and second resonance frequencies of 95Hz and 276Hz. At off-resonance frequencies, 4.5 to 7dB noise reduction is achieved with the optimally designed configuration at 287Hz. It is further seen that the control gain is not high when the closed loop is in steady state. Through experimental verification, it can be concluded that piezoelectric smart structures can be a feasible solution for cabin noise problems.

In this paper, the piezoelectric structure is attached to one side of the enclosure and the cavity shape is cubic. Since the structure is used in one direction, active noise control in the other direction may not be possible. To study the feasibility of active noise control in three dimensional space, at least three sides of the enclosure should be replaced by piezoelectric smart structures, which may result in more complicate a problem due to elasto-acoustical coupling.

References

- Clark, R.L. and Fuller, C.R., 1992, "Experiments on active control of structurally radiated sound using multiple piezoceramic actuators," *J. Acoust. Soc. Am.*, Vol. 91, No. 6, pp. 3313~3320.
- Clark, R.L. and Fuller, C.R., 1992, "Optimal Placement of Piezoelectric Actuators and Polyvinylidene Fluoride Error Sensors in Active Structural Acoustic Control Approaches," *J. Acoust. Soc. Am.*, Vol. 92, No. 3, pp. 1521~1533.
- Fahy, F., 1985, *Sound and structural vibration*, Academic press.
- Grandhi, R.V., 1989, "Structural and Control Optimization of Space Structures," *Computers & Structures*, Vol. 31 No. 2, pp. 139~150.

Hale, A.L., Lisowski, R.J. and Dahl, W.E., 1985, "Optimal Simultaneous Structural and Control Design of Maneuvering Flexible Spacecraft," *J. Guidance*, Vol. 8, No. 1, pp. 86~93.

Kim, J., 1995, *Modeling and Design of Piezoelectric Smart Structures*, Ph. D. Thesis, The Pennsylvania State University.

Kim, J., Ko, B. and Varadan, V.V., 1997, "Finite Element Modeling of Active Cabin Noise Control Problems," *4th Annual Symp. On Smart Structures & Materials* (SPIE), Vol. 3039, pp. 305~314, San Diego CA, USA.

Kim, J., Varadan, V.V. and Varadan, V.K., 1997, "Finite element modeling of structures including piezoelectric active devices," *Int. J. Num. Meth. Eng.*, Vol. 40, pp. 817~832.

Ko, B., 1996, "Active Noise Control Using Sensory Actuator," *KSME*, Vol. 20, No. 5, pp. 1573~1581

Oh, B., Lee, T., Kim, H. and Shin, J., 1993, "The Active Noise Control in Harmonic Enclosed Sound Field (I)," *KSME*, Vol. 17, No. 5, pp. 1054~1064

Wang, B-T., Burdisso, R.A. and Fuller, C.R., 1994, "Optimal Placement of Piezoelectric Actuators for Active Structural Acoustic Control," *J. Intell. Mat. Sys. Str.* Vol. 5, pp. 76~77

Varadan, V.V., Kim, J. and Varadan, V.K., 1997, "Optimal Placement of Piezoelectric Actuators for Active Noise Control," *J. of AIAA*, Vol. 35, No. 3, pp. 526~533